

Fourier transform demodulation of pixelated phase-masked interferograms

M. Servin,* J. C. Estrada, and O. Medina

Centro de Investigaciones en Optica A. C. Loma del Bosque 115, Col. Lomas del Campestre,
37150 Leon Guanajuato, Mexico

*mservin@cio.mx

Abstract: Recently a new type of spatial phase shifting interferometer was proposed that uses a phase-mask over the camera's pixels. This new interferometer allows one to phase modulate each pixel independently by setting the angle of a linear polarizer built in contact over the camera's CCD. In this way neighbor pixels may have any desired (however fixed) phase shift without cross taking. The standard manufacturing of these interferometers uses a 2x2 array with phase-shifts of 0, $\pi/2$, π , and $3\pi/2$ radians. This 2x2 array is tiled all over the video camera's CCD. In this paper we propose a new way to phase demodulate these phase-masked interferograms using the squeezing phase-shifting technique. A notable advantage of this squeezing technique is that it allows one the use of Fourier interferometry wiping out the detuning error that most phase shifting algorithms suffers. Finally we suggest the use of an alternative phase-mask to phase modulate the camera's pixels using a linear spatial carrier along a given axis.

©2010 Optical Society of America

OCIS codes: (120.3180) Interferometry; (120.2650) Fringe Analysis.

References and links

1. D. Malacara, M. Servin, and Z. Malacara, *Interferogram Analysis for Optical Testing*, 2 ed., (Taylor & Francis Group, CRC Press, 2005).
2. M. Takeda, H. Ina, and S. Kobayashi, "Fourier-transform method of fringe-pattern analysis for computer-based topography and interferometry," *J. Opt. Soc. Am. A* **72**(1), 156–160 (1982).
3. M. Servin, M. Cywiak, D. Malacara-Hernandez, J. C. Estrada, and J. A. Quiroga, "Spatial carrier interferometry from M temporal phase shifted interferograms: Squeezing Interferometry," *Opt. Express* **16**(13), 9276–9283 (2008).
4. R. Smithe, and R. Moore, "Instantaneous phase measuring interferometry," *Opt. Eng.* **23**, 361–364 (1984).
5. O. Y. Kwon, "Multichannel phase-shifted interferometer," *Opt. Lett.* **9**(2), 59–61 (1984).
6. C. L. Koliopoulos, "Simultaneous phase-shift interferometer," *Proc. SPIE* **1531**, 119–127 (1992).
7. B. K. A. Ngoi, K. Venkatakrishnan, and N. R. Sivakumar, "Phase-shifting interferometry immune to vibration," *Appl. Opt.* **40**(19), 3211–3214 (2001).
8. J. Millerd, N. Brock, J. Hayes, M. North-Morris, M. Novak, and J. C. Wyant, "Pixelated phase-mask dynamic interferometer," *Proc. SPIE* **5531**, 304–314 (2004).
9. M. Novak, J. Millerd, N. Brock, M. North-Morris, J. Hayes, and J. Wyant, "Analysis of a micropolarizer array-based simultaneous phase-shifting interferometer," *Appl. Opt.* **44**(32), 6861–6868 (2005).
10. J. F. Mosiño, M. Servin, J. C. Estrada, and J. A. Quiroga, "Phasorial analysis of detuning error in temporal phase shifting algorithms," *Opt. Express* **17**(7), 5618–5623 (2009).
11. B. T. Kimbrough, "Pixelated mask spatial carrier phase shifting interferometry algorithms and associated errors," *Appl. Opt.* **45**(19), 4554–4562 (2006).

1. Introduction

A widely used technique to demodulate fringe patterns in optical metrology is temporal Phase Shifting Interferometry (PSI) [1]. The main drawback of this technique is that it needs (for example) to piston move a reference plane to obtain a handful of phase-shifted interferograms to process. All the experimental set-up must remain "freeze" during the time required to take these temporal interferograms; this may be very difficult or even impossible. A useful alternative to temporal PSI is to obtain a spatial Linear Carrier Frequency Interferogram (LCFI) in which the Fourier demodulation technique may be used [2,3].

The standard noiseless mathematical model for a temporal interferogram is,

$$I(x, y, t) = a(x, y) + b(x, y) \cos[\phi(x, y) + \omega_0 t]. \quad (1)$$

While the one for spatial carrier (along the x axis) interferogram is,

$$I(x, y) = a(x, y) + b(x, y) \cos[\phi(x, y) + \omega_0 x]. \quad (2)$$

Where $\phi(x, y)$ is the modulating phase, $a(x, y)$ is the background, and $b(x, y)$ the contrast of the interferogram. Finally, the carrier frequency ω_0 is in radians per spatial or temporal pixel.

1.1 Four steps phase-shift demodulation of 2x2 phase-masked interferograms

To avoid the time and stability required to take several phase-shifted interferograms some researches have developed optical means to have all phase shifted images at once over the camera's light sensor [4–7]. In this direction a far more robust and compact spatial phase-shifting method has been recently developed by Millerd et al. [8,9]. In Fig. 1 we show (not showing the optical details to obtain these phase displacements [8,9]) this ingenious idea. As Fig. 1 shows, one defines a “superpixel” formed by 4 phase-shifted CCD pixels. These 4 pixels have a phase-shift of $\pi/2$ radians among them.

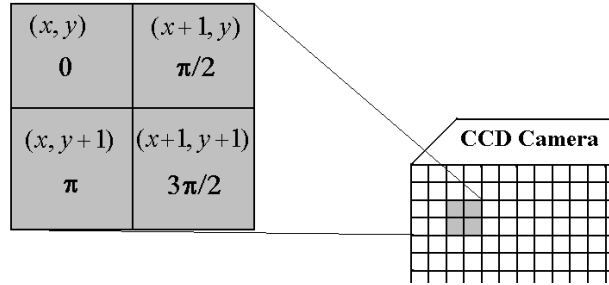


Fig. 1. This figure shows the CCD superpixel's 2x2 square array at (x, y) with a zoomed-in portion of this building block. The amount of phase shifting (in radians) introduced to each pixel is also shown.

We can sort all the 0 degrees pixels to form a 0 degree phase-shifted interferogram. The same is done for the others and obtain the 4 phase-shifted interferograms shown in Fig. 2.

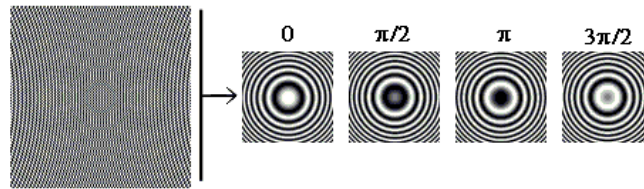


Fig. 2. Four phase-shifted interferograms obtained from the phase-masked CCD. The CCD has 128x128 pixels, and the four smaller interferograms 64x64 pixels.

Figure 2 shows four separate 64x64 pixels phase-shifted interferograms obtained from a single 128x128 simulated phase-masked CCD interferogram. Assuming that the modulating phase varies little within the 2x2 superpixel (see Fig. 1), one may use a 4-steps PSI algorithm to estimate the modulating phase of a given superpixel as,

$$\hat{\phi}(x, y) = \tan^{-1} \left[\frac{I(x, y, 0) - I(x, y+1, \pi)}{I(x+1, y, \pi/2) - I(x+1, y+1, 3\pi/2)} \right]. \quad (3)$$

The “hat” over the demodulated phase denotes its estimated value which may be a bit different from $\phi(x, y)$. These 4 pixels are not only phase-shifted but also *spatially-displaced*.

Just as a comment, the spatial impulse response associated with the 4-steps PSI algorithm in Eq. (3) is:

$$h(x, y) = \delta(x+1, y)e^{i\pi/2} + \delta(x+1, y+1)e^{i3\pi/2} + \delta(x, y) + \delta(x, y+1)e^{i\pi}. \quad (4)$$

The spatial displacement of these 4 pixels generates a significant detuning error on the estimated phase for fast spatial variations on $\phi(x, y)$. We may graphically see this error $\phi_{error}(x, y) = \hat{\phi}(x, y) - \phi(x, y)$ in Fig. 3(b), for the chirped wavefront in Fig. 3(a).

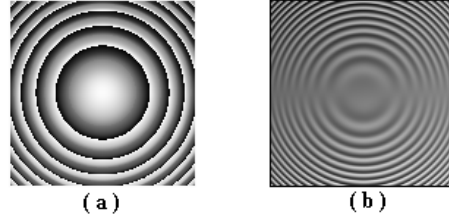


Fig. 3. In panel (a) we show the estimated phase according to Eq. (3), and in panel (b) the demodulated detuning-error $\phi_{error}(x, y)$ due to the use of this 4-steps algorithm.

The gray-level's contrast in Fig. 3(b) was multiplied by 5 for displaying purposes. This figure shows the doubling fringe-pattern phase-error associated with the 4-steps algorithm's detuning [1,8–10]. Recently however Kimbrough has improved the basic 4-step demodulating formula in Eq. (3) using N -point, class A averaging algorithm [11]. In this way he derives a complex-valued 3×3 (9-steps) convolution filter from the 2×2 (4-steps) one. Convoluting with the new 3×3 complex-valued filter one reduces the detuning error of the 4-step formula in Eq. (3) [11]. These complex-valued convolution filters demodulate all CCD pixels; just in the same way as using any other 3×3 real-valued filter [11].

Even using the 3×3 complex-valued mask as phase demodulator some detuning error remains [11]. One way to completely eliminate this detuning error is the herein proposed squeezing-Fourier phase demodulation technique.

2. Fourier Transform Demodulation (FTD) of 2×2 phase-masked interferograms

It is well known that the Fourier Transform Demodulation (FTD) technique has no detuning error [2]. This is because one completely wipes-out the right side (or the left side) of the frequency spectrum of the interferogram's real signal [10]. To obtain a single LCFI from a set of 4-phase-stepped interferograms we may use squeezing interferometry [3]. The first step in squeezing interferometry is to obtain a single LCFI as,

$$\left. \begin{aligned} I_c(4x, y) &= I(x, y, 0) \\ I_c(4x+1, y) &= I(x, y, \pi/2) \\ I_c(4x+2, y) &= I(x, y, \pi) \\ I_c(4x+3, y) &= I(x, y, 3\pi/2) \end{aligned} \right\} (0, 0) \leq (x, y) \leq (L, L). \quad (5)$$

With this technique one combines the 4 smaller $L \times L$ phase shifted interferograms (at the right hand side of Eq. (5)) into the single $4L \times L$ linear carrier fringe pattern $I_c(x, y)$ shown in Fig. 4.

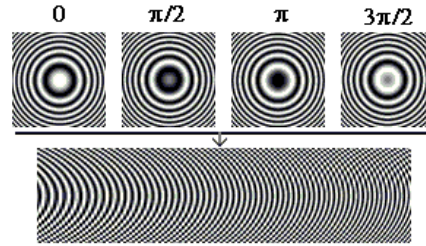


Fig. 4. Geometrical mapping (Eq. (5)) to obtain a single LCFI of size $4L \times L$ from the four smaller phase-shifted interferograms of size $L \times L$ pixels above.

We then phase demodulate the carrier frequency interferogram shown in Fig. 4 using the FTD technique and the resulting phase is shown in Fig. 5.

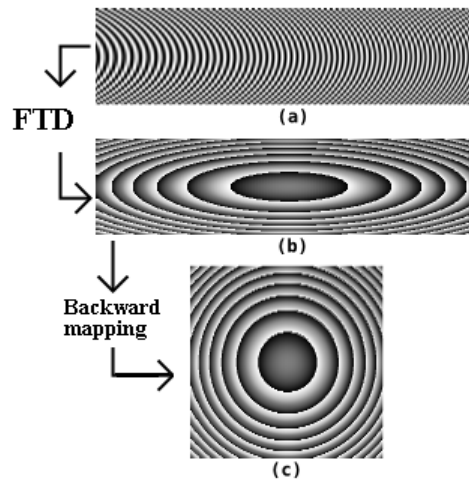


Fig. 5. Demodulation of the spatial LCFI by the FTD technique. The passing from panel (b) to panel (c) is the “backward” mapping to obtain all the camera’s CCD pixels demodulated.

The main advantage of the squeezing-FTD technique herein presented is that it has completely eliminated the spurious detuning signal from the demodulated phase [8,9]. We use the backward mapping to obtain the demodulated CCD’s pixels from the LCFI; this is shown in Fig. 5(c). This backward mapping however has a drawback. This is due to the geometrical non-continuous mapping from the LCFI to the original positions of the CCD’s pixels (see Fig. 6). This mapping error also increases as the local modulating phase-slope increases. However a big advantage is that this mapping error is of high frequency everywhere. That is because the pixels involved are from two small neighborhoods (see Fig. 6); therefore the spurious signal is high frequency. This high frequency error may be completely eliminated using a low-pass 3×3 real-valued convolution mask applied to the demodulated phase in panel 5(c). The drawback of low-pass filtering the demodulated phase is that it loses some high frequency content. In contrast the double-fringe-pattern error due to detuning is not everywhere high frequency.

3. Suggested phase-mask to obtain a linear carrier interferogram

In this section we continue analyzing the non-continuous forward-backward mapping (Fig. 6) that the squeezing-Fourier technique needs to demodulate phase-masked interferograms shown in Fig. 1. Additionally we suggest a new spatial phase-shifting mask that avoids the need of this non-continuous mapping needed by the squeezing-Fourier method.

To motivate the following discussion let us start by showing in Fig. 6, how the camera’s CCD pixels are non-continuously mapped to obtain a single LCFI.

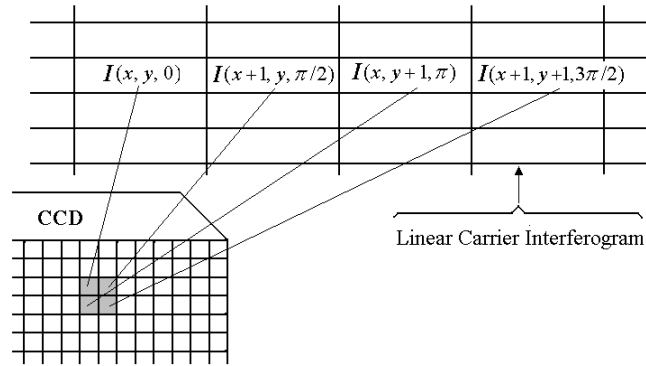


Fig. 6. Forward-backward mapping between the phase-masked CCD pixels and the LCFI. The forward mapping is the direction from the CCD to the linear carrier interferogram.

Doing this, one obtains a continuous linear phase-shift along the x direction (Fig. 4), at the expense of a non-continuous rearrangement of the spatial information in $\phi(x,y)$. That is, the quadrature filtering needed to demodulate the LCFI will smooth out the newly defined neighborhood of pixels shown in Fig. 6. Then the “backward” mapping (from panel 5(b) to panel 5(c)) generate small high-frequency phase jumps that were absent in the original CCD interferogram. These high frequency spurious phase jumps can be easily eliminated using a low pass filter over the demodulated phase. Alternatively one may low pass filter the two real-valued quadrature fringe patterns (mapped into the CCD’s geometry) obtained by the FTD technique before computing the phase in Fig. 5(c).

If however one uses the proposed phase-mask arrangement in Fig. 7 one eliminates this forward-backward non-continuous shuffling between the LCFI geometry and the CCD’s one. In this way one obtains a single carrier frequency (along the x axis) interferogram given by,

$$I(x, y) = a(x, y) + b(x, y) \cos[\phi(x, y) + (\pi / 2) x]. \quad (6)$$

This interferogram may be easily demodulated using the FTD to estimate the modulating phase $\phi(x,y)$ without accessory geometrical mapping, and without detuning. In other words, the detuning-error associated with the complex-valued 2x2 or 3x3 demodulating convolution masks [11] is completely absent due to the detuning immunity of the FTD.

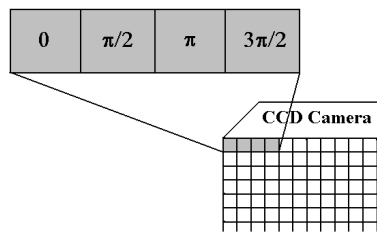


Fig. 7. Phase-mask to obtain in a direct way a standard LCFI. This mask introduces a linear carrier along the x axis of $\pi/2$ radians per pixel. As a consequence one may demodulate the LCFI obtained by the (detuning-free) FTD technique.

As far as we know, there is no clear advantage of using the detuning-sensitive complex-valued 2x2 or the less sensitive 3x3 convolution masks to demodulate the interferogram in Fig. 1, over the simpler FTD technique applied to demodulate the LCFI in Fig. 7. On the contrary, the detuning error is completely absent using the FTD technique, and we have a wealth of experience with standard linear carrier interferograms.

Before leaving this section, note that sometimes we think that the FTD technique always “over-smoothes” fast phase changes. This is only true if one makes the quadrature filter too narrow. A narrow quadrature filter attenuates much noise, and certainly over-smoothes the

demodulated phase. We may preserve the fast changes in the estimated phase if one let (almost) full-pass one side of the spectrum, for example by using the following quadrature filter:

$$H(\omega_x, \omega_y) = \begin{cases} 1 & \text{for } \omega_x < -\varepsilon \\ 0 & \text{for } \omega_x \geq -\varepsilon \end{cases} \quad (7)$$

Being ε a small real number. We do not think that the complex-valued 2x2 or 3x3 masks applied to demodulate the interferogram in Fig. 1 may have a faster phase response than the one obtained from this one-sided filter applied to an LCFI.

4. Conclusions

We have presented a new way for processing interferograms generated by phase-masked CCDs. The standard spatial modulation used in these phase-masked CCDs uses an array of 2x2 phase-shifted pixels periodically repeated all over the CCD. The squeezing-Fourier technique herein presented translates this rather unusual spatial phase modulation into a more familiar linear-carrier (along the x axis) modulation. This new spatial interferogram's rearrangement allows one to Fourier demodulate it without detuning-error [2,3]. In contrast 2x2 and 3x3 complex-valued convolution demodulators do have some detuning error [11].

Finally we have suggested a linear carrier (along the x axis) modulating phase-mask. The proposed mask in Fig. 7, allows one to phase demodulate the interferogram [8,9] using standard Fourier technique [2]. In our view, the spatial phase modulation in Fig. 1, is roughly equivalent to the spatial modulation in Fig. 7. But the benefits of demodulating a linear carrier interferogram (along a given axis) is much better understood.